

Geometry Based UAV Trajectory Planning for Mixed User Traffic in mmWave Communication

*A dissertation submitted in
partial fulfilment for the degree of*

Master of Technology

in

Computer Science

by

SK ABID HASAN

Roll no. - **CS2324**

under the supervision of

Prof. Dr. Sasthi C. Ghosh

Advanced Computing and Microelectronics Unit
(ACMU)



INDIAN STATISTICAL INSTITUTE, KOLKATA

JUNE 2025

** This work has been accepted for presentation at the IEEE International Mediterranean Conference on Communications and Networking (MeditCom 2025) at Nice, France.*

** Preprint available at [arXiv:2406.12345](https://arxiv.org/abs/2406.12345).*

** Awarded international travel grant by IEEE Communications Society for conference participation.*

Declaration

Sk Abid Hasan, with Roll No. **CS2324**, hereby declare that the material presented in the dissertation titled **Geometry Based UAV Trajectory Planning for Mixed User Traffic in mmWave Communication** represents original work carried out by me for the degree of **Master of Technology in Computer Science** at the **Indian Statistical Institute, Kolkata**.

Furthermore, I affirm that no sections of this report have been sourced or copied from external references without proper attribution. I am aware that any instances of plagiarism or the use of unacknowledged materials from third parties will be treated with the utmost seriousness and consequences.

Sk. Abid Hasan.

Sk Abid Hasan
M.Tech (CS), CS2324
Indian Statistical Institute
Kolkata – 700108, India

CERTIFICATE

This is to certify that the dissertation entitled "**Geometry Based UAV Trajectory Planning for Mixed User Traffic in mmWave Communication**" submitted by **SK ABID HASAN** to the **Indian Statistical Institute, Kolkata**, in partial fulfillment of the requirements for the degree of **Master of Technology in Computer Science**, is an authentic and genuine record of the research work carried out by the candidate under my supervision and guidance. I affirm that the dissertation has met all the necessary requirements in accordance with the regulations of this institute.



Prof. Dr. Sasthi C. Ghosh
ACMU Unit
Indian Statistical Institute
Kolkata – 700108, India

Acknowledgements

I extend my sincere appreciation to **Dr. Sasthi C. Ghosh**, my advisor at the *Advanced Computing and Microelectronics Unit* of the **Indian Statistical Institute, Kolkata**, for his guidance, continuous support, and inspiration. His profound knowledge and creative suggestions have taught me a lot about every subject and have shown me how to conduct solid research.

I would like to sincerely thank **Mr. Lakshmikanta Sau**, Senior Research Fellow at the **Indian Statistical Institute**, for his invaluable assistance in gathering the essential information for this research. His consistent provision of ideas and unwavering support have been instrumental in the success of this project.

Finally, I want to express my gratitude to my parents and extended family for their unwavering support. I also extend my sincere appreciation to all my friends for their continuous assistance and encouragement. I am thankful to everyone who has contributed to my growth and success, even if I have inadvertently missed mentioning them on the above list.

Abstract

Unmanned aerial vehicle (UAV) assisted communication is a revolutionary technology that has been recently presented as a potential candidate for beyond fifth-generation millimeter wave (mmWave) communications. Although mmWaves can offer a notably high data rate, their high penetration and propagation losses mean that line of sight (LoS) is necessary for effective communication. Due to the presence of obstacles and user mobility, UAV trajectory planning plays a crucial role in improving system performance. In this work, we propose a novel computational geometry-based trajectory planning scheme by considering the user mobility, the priority of the delay sensitive ultra-reliable low-latency communications (URLLC) and the high throughput requirements of the enhanced mobile broadband (eMBB) traffic. Specifically, we use some geometric tools like Apollonius circle and minimum enclosing ball of balls to find the optimal position of the UAV that supports uninterrupted connections to the URLLC users and maximizes the aggregate throughput of the eMBB users. Finally, the numerical results demonstrate the benefits of the suggested approach over an existing state of the art benchmark scheme in terms of sum throughput obtained by URLLC and eMBB users.

KeyWords: UAV, mmWave, URLLC, eMBB, Trajectory planning, Apollonius circle, Minimum enclosing ball.

Contents

Declaration	ii
Acknowledgements	iv
Abstract	v
1 Key Concepts and Terminologies in UAV-Aided mmWave Networks	viii
1.1 Unmanned Aerial Vehicle (UAV)	viii
1.2 Millimeter Wave (mmWave)	ix
1.3 URLLC: Ultra-Reliable Low-Latency Communication	ix
1.4 eMBB: Enhanced Mobile Broadband	x
1.5 Trajectory Planning	x
1.6 Apollonius Circle (Enclosing Circle of Three Objects)	xi
1.7 Minimum Enclosing Ball (MEB)	xi
2 Introduction	1
3 Related Work	3
4 System Model	4
4.0.1 Network Topology	4
4.0.2 Channel Model	4
4.0.3 User Traffic Characterization	5
4.0.4 UAV and UE Mobility Model	6
5 Proposed Strategy	7
5.0.1 Optimal UAV Position for URLLC Traffic	7
5.0.2 Optimal UAV Position for Both URLLC and eMBB	10
5.0.3 Complexity Analysis	12
6 NUMERICAL RESULTS	13

6.1 Simulation Results	13
7 CONCLUSION	17

Chapter 1

Key Concepts and Terminologies in UAV-Aided mmWave Networks

This chapter introduces and defines essential concepts used throughout this thesis. These terms are critical for understanding the design and analysis of UAV-based communication systems in mmWave environments.

1.1 Unmanned Aerial Vehicle (UAV)

Unmanned Aerial Vehicles (UAVs), commonly known as drones, are aircraft systems that operate without a human pilot. In wireless communication systems, UAVs are deployed as aerial base stations to dynamically enhance coverage, especially in scenarios with uneven user distribution or network congestion.

Properties:

- High mobility and flexible deployment.
- Ability to establish Line-of-Sight (LoS) communication links.
- Operate at varying altitudes depending on coverage requirements.

Advantages:

- Rapid deployment in emergency and disaster-struck areas.
- Better coverage in hard-to-reach or remote regions.
- Adaptive to user distribution and traffic demand.

Disadvantages:

- Limited battery life and payload capacity.
- Susceptible to weather conditions.
- Airspace regulations and coordination complexities.

1.2 Millimeter Wave (mmWave)

Millimeter Wave refers to the high-frequency band typically ranging from 30 to 300 GHz. mmWave enables high data rates and massive bandwidth, making it suitable for 5G and beyond. However, mmWave signals are highly susceptible to blockage and require line-of-sight (LoS) connectivity, making intelligent UAV trajectory planning essential.

Properties:

- Very high frequency and small wavelength.
- Directional transmission due to short range.
- High propagation loss and sensitivity to obstacles.

Advantages:

- Enables gigabit-per-second data rates.
- Supports dense user environments and high-throughput applications.

Disadvantages:

- Poor penetration through walls, trees, and even human bodies.
- Requires advanced beamforming and tracking mechanisms.

1.3 URLLC: Ultra-Reliable Low-Latency Communication

URLLC is one of the service categories in 5G that demands extremely low latency (as low as 1 ms) and high reliability (up to 99.999%). It supports mission-critical applications such as autonomous vehicles, factory automation, and remote surgery.

Properties:

- Strict latency and reliability constraints.
- Requires robust and redundant communication mechanisms.

Advantages:

- Enables time-sensitive and safety-critical services.
- Enhances automation and industrial process control.

Disadvantages:

- Difficult to maintain under dynamic and mobile network conditions.
- Sensitive to congestion and channel fading.

1.4 eMBB: Enhanced Mobile Broadband

eMBB is aimed at providing high-throughput connections to support applications like ultra-HD video streaming, augmented reality (AR), and virtual reality (VR). Unlike URLLC, eMBB is more tolerant to delay but requires higher data rates.

Properties:

- Designed for high data rate applications.
- Supports massive user connectivity and data consumption.

Advantages:

- Supports immersive and data-heavy applications.
- Enhances user experience in entertainment and information services.

Disadvantages:

- High data rates require more bandwidth and energy.
- Challenging to serve in edge or rural areas with low infrastructure.

1.5 Trajectory Planning

Trajectory planning refers to computing the optimal flight path for a UAV to meet specific objectives such as maximizing coverage, maintaining connectivity, or minimizing energy consumption. In mmWave communications, trajectory planning is particularly important due to the directional nature of the antennas and LoS constraints.

Properties:

- Often formulated as an optimization problem.
- Depends on user density, mobility, and traffic demands.

Advantages:

- Improves overall network performance and quality of service.
- Minimizes energy usage and prolongs UAV flight time.

Disadvantages:

- Computationally expensive in dynamic environments.
- Must consider obstacles, interference, and user mobility.

1.6 Apollonius Circle (Enclosing Circle of Three Objects)

The Apollonius circle is defined as a circle that is tangent to three given circles in the plane, with up to eight such solutions possible based on combinations of internal and external tangency. Among these, this work specifically utilizes the unique Apollonius circle that externally and tangentially encloses all three given circles. This outer Apollonius circle ensures complete coverage of the three regions, making it ideal for UAV placement where simultaneous service to spatially distributed users is required. The geometric properties of this circle—its center and radius—are used to determine optimal UAV hover locations. The construction employs classical inversion techniques to derive the desired solution efficiently. This choice offers both geometric simplicity and practical relevance in coverage-oriented network designs. Degeneracies may arise when the input circles are not in general position.

1.7 Minimum Enclosing Ball (MEB)

The Minimum Enclosing Ball (MEB) of a set of points is the smallest ball (or circle in 2D) that contains all the points. It is widely used in UAV coverage problems to identify the minimal area required to cover a cluster of users. The MEB's center is a good candidate for UAV placement to ensure coverage with minimal power consumption or beam divergence.

Chapter 2

Introduction

With the development of communication technologies, wireless communication is becoming the backbone of daily life. Because of their low acquisition costs, ease of deployment, and hovering capabilities, unmanned aerial vehicles (UAVs) are seen as a promising solution to meet ever-increasing traffic demands, improve coverage area, and avoid obstacles [9]. UAV-assisted millimeter wave (mmWave) communication is an appealing option to meet these growing demands because of its high bandwidth and an enormous amount of unoccupied spectrum. However, due to very high frequency, mmWaves suffer from its own set of shortcomings like significantly high penetration and propagation losses, resulting in connection failure in the presence of obstacles[18]. According to the data requirements and delay sensitivity, there are mainly three different types of user traffic: enhanced mobile broadband (eMBB), ultra-reliable low-latency communications (URLLC), and massive machine-type communications (mMTC) [14, 4]. Since mMTCs is about wireless connectivity to tens of billions of machine-type terminals, here, we consider cost-efficient URLLCs and eMBB traffic that is adequate for human-type cellular communications [4]. The main focus of this manuscript is to develop a UAV trajectory planning that takes into account the user's traffic characteristics and mobility.

In this manuscript, we propose a UAV trajectory planning technique to serve the users by considering their traffic characteristics and mobility in the presence of obstacles. Specifically, due to the delay sensitivity of the URLLC traffic, we consider that a maximum number of URLLC users must be served. On the other hand, since eMBB traffic is susceptible to minor disruptions, we maximize the aggregate throughput of eMBB users while ensuring that the maximum number of URLLC users is being served. Here, we use some basic computational geometry concepts, like the Apollonius circle and minimum enclosing ball of balls, to predict the appropriate UAV location for the

next time instant to meet the desired objective. More specifically, our contributions are as follows:

- In order to serve maximum URLLC users, we find the Apollonius circle or minimum enclosing ball of balls and hence the probable zone for UAV location. Thereafter, discretizing that zone, we identify a set of potential candidate locations for UAV positioning, which can provide LoS links to all the probable positions of the URLLC users.
- Next, after finding the zone for URLLC users, we move the UAV to a point within that zone from where the eMBB users get maximum aggregate throughput.
- If we get more than one such point, we move the UAV to that point for which the displacement with respect to the previous location of the UAV is minimum.

We performed extensive simulations to demonstrate the benefits of the suggested approach over an existing state of the art benchmark scheme in terms of the sum throughput obtained by both URLLC and eMBB users.

Chapter 3

Related Work

In UAV-assisted air-to-ground (A2G) communication, direct line of sight (LoS) links may be blocked due to the presence of obstacles. The authors in [2], proposed a path loss model for both LoS and non-LoS (NLoS) communication, but in case of mmWave communications due to higher path-loss, the NLoS links are almost infeasible[16]. The authors in [10], use a sigmoid function to model the probability of LoS to a user, characterize the UAV's coverage radius as a function of path loss, and show how optimizing the coverage radius in an interference-free environment can maximize the UAV height. The coverage analysis for low-altitude UAV networks in urban areas has been investigated well in [8]. However, both [10] and [8] considered that the users are static. In [5], the authors proposed an optimal UAV placement technique with respect to power loss and overall outage by considering both users and obstacles to be static. However, in most of the practical scenarios, users may not be static in nature [3]. Moreover, in [13], the authors proposed an optimization-based UAV placement strategy by considering the achievable data rate of the users. However, they did not consider the presence of obstacles and assumed LoS links are always available to the ground users. Furthermore, the authors of [20] and [21] gave a beautiful insight into power control and energy-efficient trajectory planning. However, they also did not consider the aspect of user mobility. A joint power control and optimal placement techniques have been proposed in [15] considering static URLLC users only. The authors of [12] proposed a trajectory planning algorithm without considering the impact of user's traffic characteristics. To the best of our knowledge, this is the first work that considers heterogeneous user traffic characteristics along with user mobility for UAV trajectory planning in the presence of obstacles.

Chapter 4

System Model

Here we discuss both the considered network topology as well as the mathematical construction of the problem.

4.0.1 Network Topology

We consider an A2G cellular wireless communication system that consists of m number of user equipments (UEs) d_1, \dots, d_m , k number of UAVs u_1, u_2, \dots, u_k , and n number of randomly located static obstacles. Additionally, we assume that each UE and UAV consists of a single and l number of antennas, respectively, and all the UAVs are connected with a macro base station (BS) B through a backhaul network. Note that UAVs are designed as multiple aerial BSs that can serve a maximum l number of UEs at a time. However, in a particular time instance, each UE is connected with at most one UAV. Furthermore, we also assume that the coverage area and flying height of a UAV are R and h , respectively. The system model is demonstrated in Fig. 4.1.

4.0.2 Channel Model

In our considered topology, UAVs, and UEs are mobile in nature. As a result, due to the presence of static obstacles, the direct LoS may be blocked by the obstacles. Therefore, the transmitted signals from UAV reach UE via the LoS and NLoS links. Due to the high path loss at mmWave frequencies, we consider only LoS links for successful communication. Let us consider that, for a particular $u_i - d_j$ link, depending on the 73 GHz model, the path loss (in dB) is modeled as [1]

$$PL_{i,j}(d_{i,j})[dB] = \alpha + 10\beta \log_{10}(d_{i,j}), \quad (4.1)$$

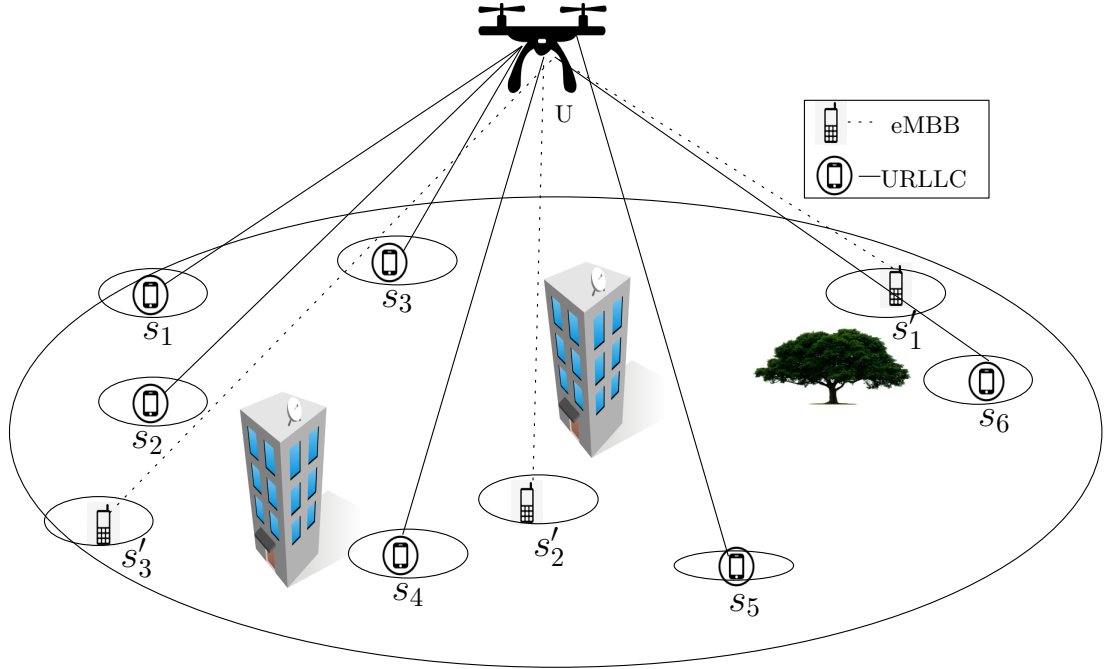


Figure 4.1: Communication Environment

where α and β are environment-specific constants that characterize signal attenuation, and $d_{i,j}$ is Euclidian distance between u_i and d_j . Now, the received power at d_j , in dBm , is computed using the link budget equation;

$$P_{i,j}[dBm] = P_i + G_i + G_j - PL_{i,j}(d_{i,j}), \quad (4.2)$$

where P_i is the transmit power, G_i and G_j are the antenna gains of u_i and d_j respectively. Therefore, the corresponding throughput at user d_j for UAV u_i is [1]

$$T_{i,j} = B_w \log_2 \left(1 + \frac{P_{i,j} \times |g_{i,j}|^2}{\sigma_0} \right), \quad (4.3)$$

where B_w is channel bandwidth, σ_0^2 is the variance of the circularly symmetric zero mean additive white Gaussian noise and $|g_{i,j}|$ is the Rician random variable depending on whether it corresponds to LoS model [17]. Note that, here, we assume orthogonal frequency division multiple access (OFDMA) where each UE communicates using orthogonal resource blocks [19].

4.0.3 User Traffic Characterization

In our considered network topology, according to the user's delay tolerance, we characterize the user traffic in two separate scenarios, namely eMBB and URLLC. Note that URLLC traffic is designed for very low latency and high-reliability applications,

enabling real-time mission-critical communication where even a minor delay or packet loss can lead to failures or catastrophic consequences. However, eMBB traffic is designed to provide high-speed, high-capacity, and data-intensive applications. Unlike URLLC, eMBB applications can tolerate minor delays without causing critical failures. Here we focus on URLLCs and eMBB traffic that is adequate for human-type cellular and wireless communication, keeping mMTCs outside the scope of this manuscript.

4.0.4 UAV and UE Mobility Model

For a duration of Δt time, we assume that both UAVs and UEs move according to random waypoint mobility model [3]. However, their positions and velocities are measured at the beginning of Δt and the velocities are assumed to be fixed throughout that Δt . The velocity ranges of d_i and u_i are $v_i \in (0, v_{\max})$ and $v'_i \in (0, v'_{\max})$, respectively. Here v_{\max} and v'_{\max} are the maximum velocities of UEs and UAVs respectively, where $v_{\max} \leq v'_{\max}$. Since the height of UAV is assumed to be remain fixed, during Δt time, both d_i and u_i will stay within the disks of radii $v_i\Delta t$ and $v'_i\Delta t$ centered on their positions at the start of Δt in the appropriate \mathbb{R}^2 planes, one at ground level for users and the other one at UAV height h , respectively.

Chapter 5

Proposed Strategy

In this section, we propose a trajectory planning algorithm for UAV u based on both URLLC and eMBB traffic. Specifically, first, we propose an algorithm to identify a zone from where the highest number of URLLC users will be covered by u . Next, we propose an algorithm to find the final location of u within the identified zone, which serves the maximum amount of eMBB traffic. The complete process is described below.

5.0.1 Optimal UAV Position for URLLC Traffic

Let \mathcal{S} be the set of all URLLC users that are being served by u at a particular time instance $t = t_0$ and their corresponding positions are given by

$$e_i = (x_i, y_i), \quad i = 1, \dots, |\mathcal{S}|, \quad (5.1)$$

where $|\mathcal{S}|$ denotes the cardinality of \mathcal{S} . Additionally, we consider that $e_0 = (x_0, y_0)$ is the position of u at $t = t_0$. Due to the mobile nature of the user $s_i \in \mathcal{S}$, according to Section 4.0.4, s_i lies within a disk of radius $v_i\Delta t$ during t_0 to $t_0 + \Delta t$, where v_i is the velocity of s_i . Here, we denote the disk within which $s_i \in \mathcal{S}$ can lie as

$$\mathcal{D}_i = \{(x, y) : (x - x_i)^2 + (y - y_i)^2 \leq (v_i\Delta t)^2\}. \quad (5.2)$$

Similarly, u may lie inside a disk \mathcal{A} of radius $v'\Delta t$, with e_0 at its center, during t_0 to $t_0 + \Delta t$. That is,

$$\mathcal{A} = \{(x, y) : (x - x_0)^2 + (y - y_0)^2 \leq (v'\Delta t)^2\}, \quad (5.3)$$

where v' is the velocity of u . We now formally define when s_i is said to be coverable and covered by u .

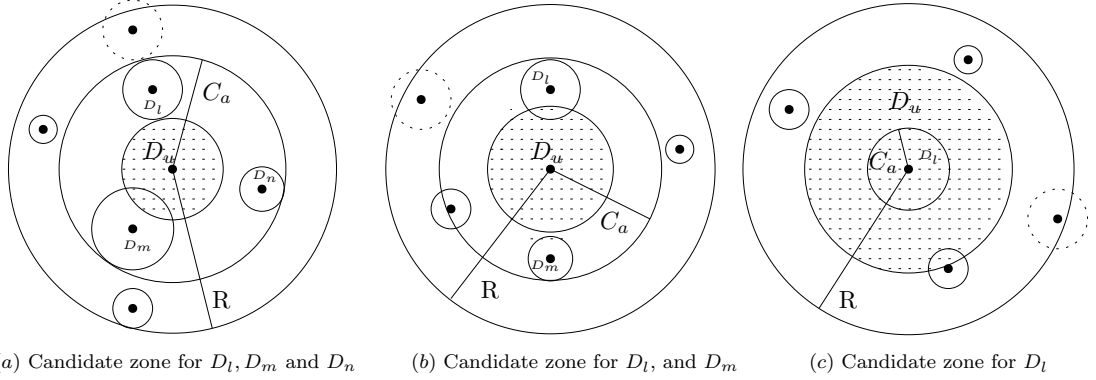


Figure 5.1: Candidate zone for URLLC traffic

Coverable: A user $s_i \in \mathcal{S}$ located at e_i is said to be coverable by u located at p , if the Euclidean distance between them, $d(p, e_i) \leq R - (v_i \Delta t)$.

Covered: A user $s_i \in \mathcal{S}$ located at e_i is said to be covered by u located at p , if:

1. s_i is coverable by u , and
2. $\forall q \in \mathcal{D}_i, \exists$ a LoS between p and q , and the achievable data rate obtained by s_i located at q from u is greater than the minimum data rate threshold $R_{\text{req}}(s_i)$ of s_i .

From computational geometry, if \mathcal{C} is a set of d -dimensional balls, there exists $\mathcal{E} \subset \mathcal{C}$ with at most $(d + 1)$ balls such that the minimum enclosing ball of \mathcal{E} equals that of \mathcal{C} , i.e., $\text{MB}(\mathcal{E}) = \text{MB}(\mathcal{C})$, where $\text{MB}(\cdot)$ denotes the minimum enclosing ball [7]. The Apollonius circle \mathcal{C}_a [6] of three circles is the minimum radius circle that contains all three circles and is tangent to each of them. With the help of \mathcal{C}_a , we find the region for u that covers the maximum number of $s_i \in \mathcal{S}$ as described below. Let $\mathcal{D}_l, \mathcal{D}_m$ and \mathcal{D}_n be three coverable disks with radii r_l, r_m and r_n with respect to s_l, s_m and $s_n \in \mathcal{S}$, respectively. The center and radius of the Apollonius circle \mathcal{C}_a corresponding to $\mathcal{D}_l, \mathcal{D}_m$ and \mathcal{D}_n are (h, k) and r_a , respectively (Fig. 5.1(a)). From \mathcal{C}_a and \mathcal{D}_w , we obtain:

$$(h - x_w)^2 + (k - y_w)^2 = (r_a - r_w)^2, \quad w = l, m, n. \quad (5.4)$$

We define a function A_{ovl} that provides an overlapping region between two disks. For two disks:

$$\mathcal{X}_i = \{(x, y) : (x - p_i)^2 + (y - q_i)^2 \leq r_i^2\}, \quad i \in \{1, 2\}, \quad (5.5)$$

$A_{\text{ovl}}(\mathcal{X}_1, \mathcal{X}_2)$ is computed as:

$$A_{\text{ovl}}(\mathcal{X}_1, \mathcal{X}_2) = r_1^2 \cos^{-1} \left(\frac{d^2 + r_1^2 - r_2^2}{2dr_1} \right) + r_2^2 \cos^{-1} \left(\frac{d^2 + r_2^2 - r_1^2}{2dr_2} \right) - \eta, \quad (5.6)$$

where $d = \sqrt{(p_2 - p_1)^2 + (q_2 - q_1)^2}$ and

$$\eta = \frac{1}{2} \sqrt{(-d + r_1 + r_2)(d - r_1 + r_2)} \times \sqrt{(d + r_1 - r_2)(d + r_1 + r_2)}. \quad (5.7)$$

Let \mathcal{D}_u be the region with center (h, k) and radius $R - r_a$ that satisfies:

$$R \geq r_a, \quad (5.8)$$

$$A_{\text{ovl}}(\mathcal{A}, \mathcal{D}_u) > 0. \quad (5.9)$$

We discretize $\mathcal{D}_u \cap \mathcal{A}$ into unit grids. Let $\mathcal{D}_u(l, m, n)$ be the set of all grid centers that cover $\mathcal{D}_l, \mathcal{D}_m$ and \mathcal{D}_n :

$$\mathcal{D}_u(l, m, n) = \{z \in \mathcal{D}_u \cap \mathcal{A} : \mathcal{D}_l, \mathcal{D}_m, \mathcal{D}_n \text{ covered from } z\}. \quad (5.10)$$

The potential candidate zone of u is:

$$\mathcal{Z} = \bigcup_{\substack{1 \leq l, m, n \leq |\mathcal{S}| \\ l \neq m \neq n}} \mathcal{D}_u(l, m, n). \quad (5.11)$$

We construct a binary matrix $M = (M_{ij})_{|\mathcal{S}| \times |\mathcal{Z}|}$ where:

$$M_{ij} = \begin{cases} 1, & \text{if } s_i \text{ is covered from } z_j, \\ 0, & \text{otherwise.} \end{cases} \quad (5.12)$$

The column sum $S(z_j) = \sum_{i=1}^{|\mathcal{S}|} M_{ij}$ gives the number of users covered from z_j . The optimal location is:

$$\mathcal{Z}_u = \{z_j \in \mathcal{Z} : S(z_j) = \max_{z_k \in \mathcal{Z}} S(z_k)\}. \quad (5.13)$$

If no triplets satisfy the conditions, we repeat the process for pairs and individual disks

using the minimum enclosing ball C_{MB} (Fig. 5.1). The complete process is described in Algorithm 1.

Algorithm 1 Optimal UAV Position for URLLC Traffic

Require: $\mathcal{S}, \mathcal{A}, \mathcal{D} = \{\mathcal{D}_i \mid s_i \in \mathcal{S}\}$

Ensure: \mathcal{Z}_u

```

1: Initialize  $\mathcal{Z} \leftarrow \emptyset, \mathcal{Z}_u \leftarrow \emptyset$ 
2: for all triplets  $\mathcal{D}_l, \mathcal{D}_m, \mathcal{D}_n \in \mathcal{D}$  with  $l \neq m \neq n$  do
3:   Compute  $\mathcal{C}_a$  and  $\mathcal{D}_u$ 
4:   if  $r_a \leq R$  and  $A_{\text{ovl}}(\mathcal{A}, \mathcal{D}_u) > 0$  then
5:     Compute potential zone  $\mathcal{D}_u(l, m, n)$ 
6:      $\mathcal{Z} \leftarrow \mathcal{Z} \cup \mathcal{D}_u(l, m, n)$ 
7:   end if
8: end for
9: if  $\mathcal{Z} = \emptyset$  then
10:  for all pairs  $\mathcal{D}_l, \mathcal{D}_m \in \mathcal{D}$  with  $l \neq m$  do
11:    Compute  $C_{\text{MB}}$  and  $\mathcal{D}_u$ 
12:    if  $r_{\text{MB}} \leq R$  and  $A_{\text{ovl}}(\mathcal{A}, \mathcal{D}_u) > 0$  then
13:      Compute potential zone  $\mathcal{D}_u(l, m)$ 
14:       $\mathcal{Z} \leftarrow \mathcal{Z} \cup \mathcal{D}_u(l, m)$ 
15:    end if
16:  end for
17:  if  $\mathcal{Z} = \emptyset$  then
18:    for all  $\mathcal{D}_l \in \mathcal{D}$  do
19:      Compute  $\mathcal{D}_u$ 
20:      if  $A_{\text{ovl}}(\mathcal{A}, \mathcal{D}_u) > 0$  then
21:        Compute potential zone  $\mathcal{D}_u(l)$ 
22:         $\mathcal{Z} \leftarrow \mathcal{Z} \cup \mathcal{D}_u(l)$ 
23:      end if
24:    end for
25:  end if
26: end if
27: Construct matrix  $M$  where  $M_{ij} = 1$  if  $s_i$  is covered from  $z_j$ 
28: Compute column sums  $S(z_j) = \sum_{i=1}^{|\mathcal{S}'|} M_{ij}$ 
29:  $\mathcal{Z}_u \leftarrow \{z_j \in \mathcal{Z} : S(z_j) = \max S(z_k)\}$ 
30: return  $\mathcal{Z}_u$ 

```

5.0.2 Optimal UAV Position for Both URLLC and eMBB

Let \mathcal{S}' be the set of eMBB users served by u at $t = t_0$ with positions:

$$e'_i = (x'_i, y'_i), \quad i = 1, \dots, |\mathcal{S}'|. \quad (5.14)$$

The disk within which $s'_i \in \mathcal{S}'$ can lie during $(t_0, t_0 + \Delta t)$ is:

$$\mathcal{D}'_i = \{(x, y) : (x - x'_i)^2 + (y - y'_i)^2 \leq (v'_i \Delta t)^2\}, \quad (5.15)$$

where v'_i is the velocity of s'_i .

Let $\mathcal{D}_o(iz) = A_{\text{ovl}}(\mathcal{D}'_i, \mathcal{A}_z)$ be the overlap between \mathcal{D}'_i and \mathcal{A}_z (radius R centered at $z \in \mathcal{Z}_u$). Discretizing $\mathcal{D}_o(iz)$ into grids, the throughput T_{iz} obtained by s'_i from z is:

$$T_{iz} = \frac{\sum_{w \in \mathcal{D}_o(iz)} T(wz)}{|\mathcal{D}_o(iz)|}, \quad (5.16)$$

where $T(wz)$ is computed using (4.3). The total eMBB throughput from z is:

$$T(z) = \sum_{i=1}^{|\mathcal{S}'|} T_{iz}. \quad (5.17)$$

The optimal position $z^* \in \mathcal{Z}_u$ maximizes $T(z)$. If multiple positions yield the same throughput, we select the one closest to e_0 . The complete process is described in Algorithm 2.

Algorithm 2 Final Position Selection for eMBB Traffic

Require: $\mathcal{Z}_u, \mathcal{S}'$

Ensure: z^*

- 1: **for** each $z \in \mathcal{Z}_u$ **do**
 - 2: **for** each $s'_i \in \mathcal{S}'$ **do**
 - 3: Compute $\mathcal{D}_o(iz)$
 - 4: **for** each grid center $w \in \mathcal{D}_o(iz)$ **do**
 - 5: Compute $T(wz)$ using (4.3)
 - 6: **end for**
 - 7: $T_{iz} \leftarrow \frac{\sum_w T(wz)}{|\mathcal{D}_o(iz)|}$
 - 8: **end for**
 - 9: $T(z) \leftarrow \sum_{i=1}^{|\mathcal{S}'|} T_{iz}$
 - 10: **end for**
 - 11: $T^* \leftarrow \max_{z \in \mathcal{Z}_u} T(z)$
 - 12: $\mathcal{Z}'_u \leftarrow \{z \in \mathcal{Z}_u : T(z) = T^*\}$
 - 13: **if** $|\mathcal{Z}'_u| > 1$ **then**
 - 14: $z^* \leftarrow \underset{z \in \mathcal{Z}'_u}{\text{argmin}} d(e_0, z)$
 - 15: **else**
 - 16: $z^* \leftarrow$ the single element in \mathcal{Z}'_u
 - 17: **end if**
 - 18: **return** z^*
-

5.0.3 Complexity Analysis

A UAV u can provide services to at most l UEs at a particular time slot. That is, $|S| + |S'| \leq l$. Let r be the maximum radius among all the users in $S \cup S'$ and r' be the radius of disk A . Discretizing two circles of radii r and r' into unit cells and then checking LoS status between every pair cells, requires $O(r'^2 r^2)$ time complexity. The time and space complexity of the proposed algorithms are as follows:

- **Algorithm 1:**

- Time: $O(l^3 \cdot r'^2 \cdot r^2)$ (worst-case, checking all triplets)
- Space: $O(r'^2 \cdot l)$ (storing coverage matrix)

- **Algorithm 2:**

- Time: $O(l \cdot r'^2 \cdot r^2)$ (evaluating all candidate positions)
- Space: $O(r'^2 \cdot l)$ (storing throughput values)

Chapter 6

NUMERICAL RESULTS

6.1 Simulation Results

In this section, our main goal is to assess how well the suggested approach works in different environmental settings. We have included a performance comparison study against an existing approach [12]. In [12], a trajectory planning is obtained by taking into account the mobility of users and the obstacles in their environment, without considering the influence of user traffic characteristics. The objective of our proposed approach is to optimize the sum throughput obtained by both URLLC and eMBB users while serving a maximum number of URLLC users. The simulation parameters that we used are given in Table 6.1

Parameter	Value
Communication region	$400m \times 400m$
Coverage Radius (R)	$46m$
Time slot duration (Δt)	3 sec
Transmission power (P_i)	30 dBm [16]
Gain of the transmit antenna	$G_{x_m} = 24.5$ dBi [16]
Gain of the receive antenna	$G_{y_m} = 24.5$ dBi [16]
URLLC threshold (R_{req})	10 Mbps [ITU & 3GPP]
Rician fading factor (K)	2 [16]
Altitude of UAV	[22 m, 150 m] [11]
Carrier frequency	73 GHz [1]
LoS link parameters	$\alpha = 69.8, \beta = 2$ [1]

Table 6.1: Simulation Parameters

Fig.6.1 shows a comparison of eMBB throughput, URLLC throughput, and sum

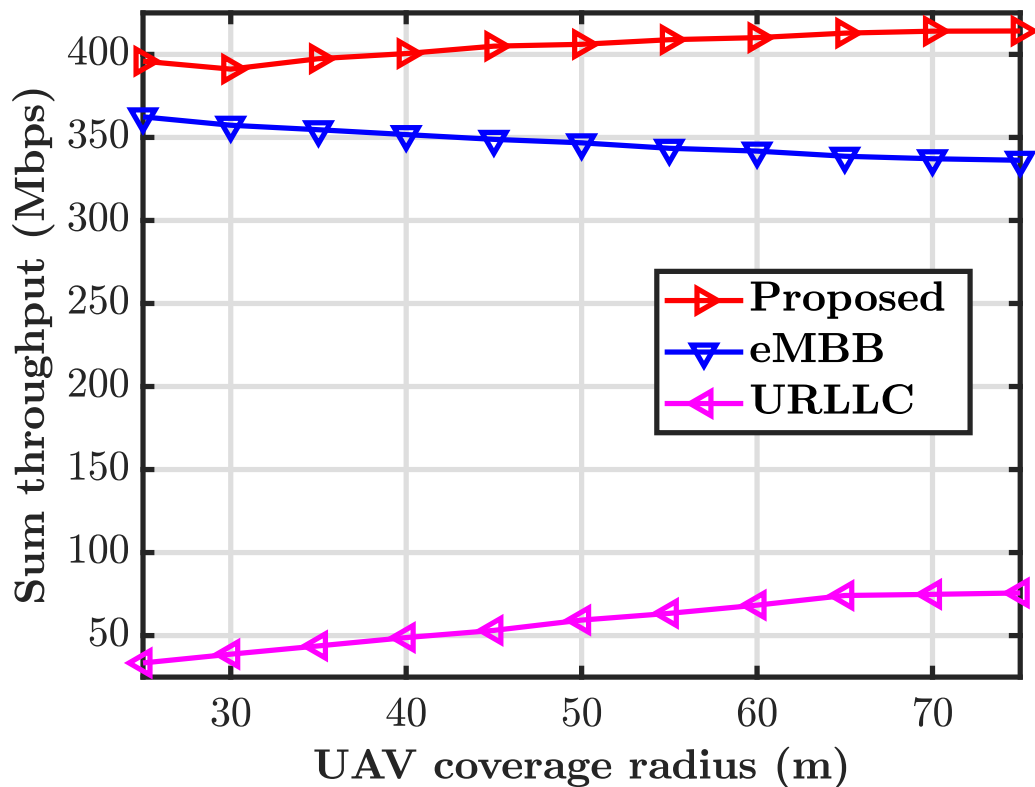


Figure 6.1

throughput obtained by our proposed algorithm for different UAV coverage radii. Here eMBB and URLLC throughputs represent the aggregate throughputs obtained by the eMBB and URLLC users respectively. Sum throughput (Proposed) represents the sum of eMBB and URLLC throughputs. Note that the coverage radius of the UAV is increased in Fig 6.1 up to the limit such that the minimum data rate requirement of the URLLC users is satisfied. Hence the URLLC throughput increases with the increase of UAV coverage radius. On the contrary, as the UAV coverage radius increases, throughputs obtained by the eMBB users decrease as achievable throughput is inversely proportional to the distance from the user to the UAV. Since URLLC is highly prioritized, the increment of URLLC throughput is slightly more than the decrement of eMBB throughput. Hence sum throughput has an increasing trend.

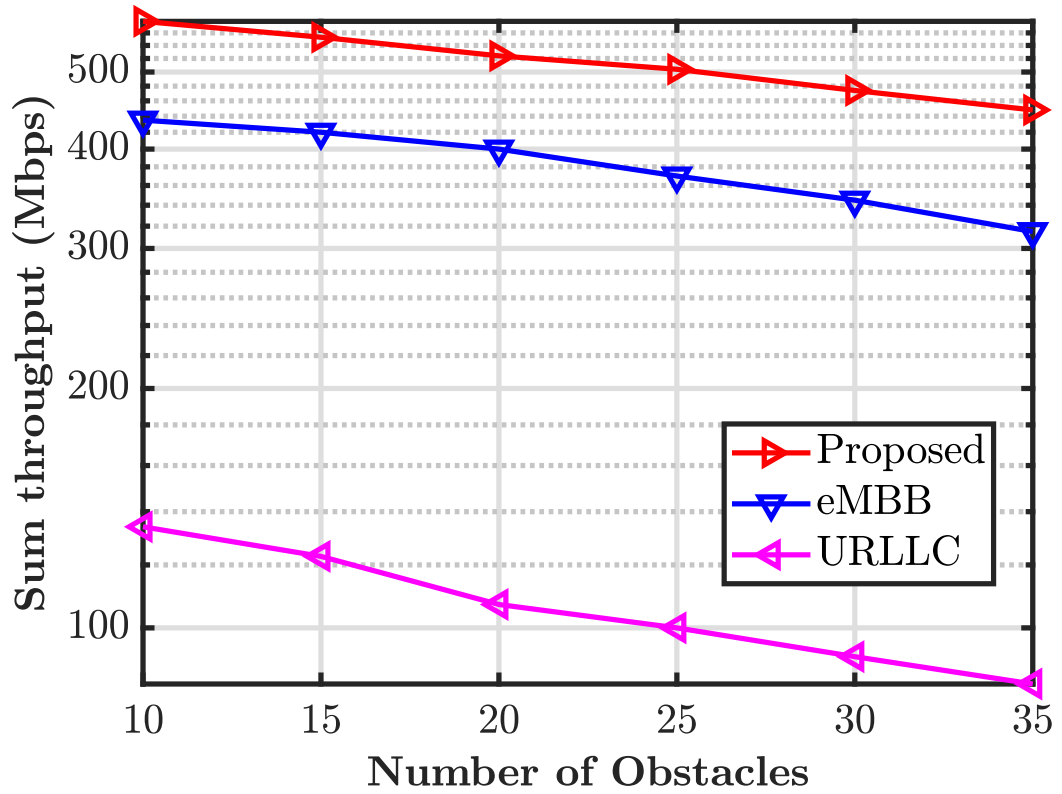


Figure 6.2

Furthermore, Fig. 6.2 investigates the impact of obstacle density on the sum throughput, eMBB throughput, and URLLC throughput for a fixed number of users (35). As obstacle density increases, the possibility of having LoS decreases. Thus all the throughputs decrease. Note that URLLC users are considered to be covered if all the points in its disk get LoS and eMBB users can be covered partially. That's why we observe that URLLC throughput decreases more rapidly than the eMBB throughput. Accordingly, the sum throughput is also decreasing as a combined effect of both of them.

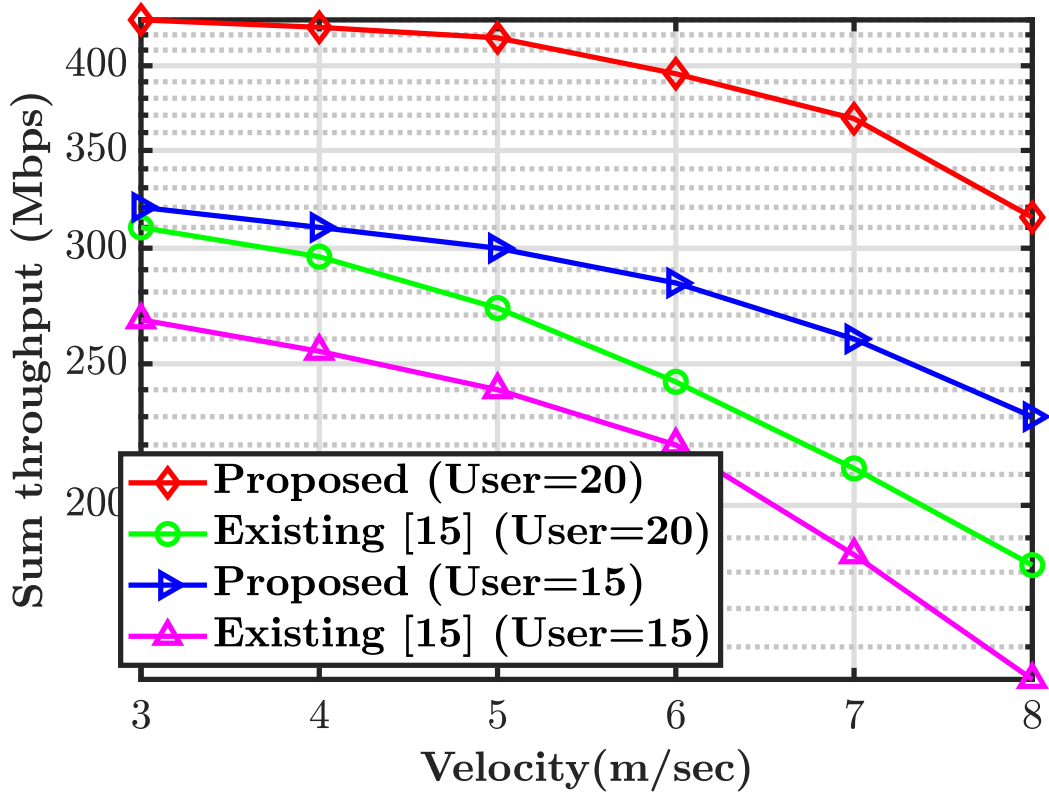


Figure 6.3

Finally, Fig.6.3 presents a comparative analysis between the proposed strategy and the existing scheme [12] under varying user velocities, for a fixed number of users (15 and 20). It is observed that our approach significantly outperforms the method described in [12]. The key reason behind this improvement is the differentiated treatment of URLLC and eMBB users based on their inherent service requirements, unlike [12] which treats all users uniformly. Specifically, due to the ultra-reliability and low-latency demands of URLLC, our method prioritizes serving as many URLLC users as possible. Subsequently, from that UAV position, we aim to maximize the service for eMBB users by leveraging partial coverage, acknowledging that eMBB users can tolerate moderate latency or brief service interruptions. In contrast, the approach in [12] treats all users as URLLC, meaning that eMBB users also receive low-latency, ultra-reliable service, resulting in inefficient use of network resources. This performance gap is clearly reflected in the figure. Moreover, we observe that our strategy yields more consistent results than [12] across varying user velocities, demonstrating its robustness and adaptability to different environmental conditions.

Chapter 7

CONCLUSION

In this work, we investigated the impact of user and UAV mobility on system performance in an air-to-ground mmWave communication framework, considering mixed user traffic types such as URLLC and eMBB. We proposed a geometry-driven UAV trajectory planning algorithm that utilizes the Apollonius circle and the minimum enclosing ball of balls to determine optimal UAV deployment locations. The approach emphasizes maintaining line-of-sight connectivity and effective user coverage under traffic-specific constraints. Numerical evaluations demonstrated that our proposed strategy significantly outperforms an existing benchmark in terms of overall system throughput. These results highlight the effectiveness of geometry-based heuristics in achieving high performance in dynamic and heterogeneous wireless environments.

Bibliography

- [1] M. R. Akdeniz et al. “Millimeter wave channel modeling and cellular capacity evaluation”. In: *IEEE J. Sel. Areas Commun.* 32.6 (June 2014), pp. 1164–1179.
- [2] M. Alzenad et al. “3-D Placement of an Unmanned Aerial Vehicle Base Station (UAV-BS) for Energy-Efficient Maximal Coverage”. In: *IEEE Wireless Commun. Lett.* 6.4 (Aug. 2017), pp. 434–437.
- [3] C. Bettstetter, G. Resta, and P. Santi. “The node distribution of the random waypoint mobility model for wireless ad hoc networks”. In: *IEEE Trans. Mob. Comput.* 2.3 (July 2003), pp. 257–269.
- [4] C. Bockelmann et al. “Massive machine-type communications in 5G: Physical and MAC-layer solutions”. In: *IEEE Commun. Mag.* 54.9 (Oct. 2016), pp. 59–65.
- [5] Y. Chen, W. Feng, and G. Zheng. “Optimum placement of UAV as relays”. In: *IEEE Commun. Lett.* 22.2 (Feb. 2018), pp. 248–251.
- [6] H. Coxeter. “The problem of Apollonius”. In: *Amer. Math. Monthly* 75.1 (1968), pp. 5–15.
- [7] K. Fischer and B. Gartner. “The smallest enclosing ball of balls: combinatorial structure and algorithms”. In: *in Proc. 19th Annu. Symp. on Comput. Geom.* 2003, pp. 292–301.
- [8] B. Galkin, J. Kibilda, and L. A. DaSilva. “Coverage analysis for low-altitude UAV networks in urban environments”. In: *in Proc. IEEE Global Commun. Conf. (GLOBECOM)*. 2017, pp. 1–6.
- [9] L. Gupta, R. Jain, and G. Vaszkun. “Survey of important issues in UAV communication networks”. In: *IEEE Commun. Surv. Tutorial* 18.2 (2015), pp. 1123–1152.
- [10] A. Al-Hourani, S. Kandeepan, and S. Lardner. “Optimal LAP altitude for maximum coverage”. In: *IEEE Wireless Commun. Lett.* 3.6 (June 2014), pp. 569–572.
- [11] F. Li et al. “Geometric analysis-based 3D anti-block UAV deployment for mmWave communications”. In: *IEEE Commun. Lett.* 26.11 (Nov. 2022), pp. 2799–2803.

- [12] G. Li et al. “A UAV Real-time Trajectory Optimized Strategy for Moving Users”. In: *Proc. 11th Int. Conf. Wireless Commun. Signal Process. (WCSP)*. IEEE, 2019, pp. 1–6. DOI: [10.1109/WCSP.2019.8927863](https://doi.org/10.1109/WCSP.2019.8927863).
- [13] L. Liu, S. Zhang, and R. Zhang. “CoMP in the sky: UAV placement and movement optimization for multi-user communications”. In: *IEEE Trans. Commun.* 67.8 (Aug. 2019), pp. 5645–5658.
- [14] P. Popovski et al. “5G wireless network slicing for eMBB, URLLC, and mMTC: A communication-theoretic view”. In: *IEEE Access* 6 (2018), pp. 55765–55779.
- [15] H. Ren et al. “Joint transmit power and placement optimization for URLLC-enabled UAV relay systems”. In: *IEEE Trans. Veh. Technol.* 69.7 (July 2020), pp. 8003–8007.
- [16] L. Sau, P. Mukherjee, and S. C. Ghosh. “DRAMS: Double-RIS assisted multihop routing scheme for device-to-device communication”. In: *Comput. Commun.* 220 (Apr. 2024), pp. 52–63.
- [17] L. Sau, P. Mukherjee, and S. C. Ghosh. “Priority-aware grouping-based multihop routing scheme for RIS-assisted wireless networks”. In: *IEEE Trans. Network Sci. Eng.* 12.2 (Mar. 2025), pp. 1172–1185.
- [18] X. Wang et al. “Millimeter wave communication: A comprehensive survey”. In: *IEEE Commun. Surv. Tutorials* 20.3 (2018), pp. 1616–1653.
- [19] T. Weiss et al. “Mutual interference in OFDM-based spectrum pooling systems”. In: *2004 IEEE 59th Veh. Technol. Conf.* Vol. 4. 2004, pp. 1873–1877.
- [20] H. Yan, Y. Chen, and S.-H. Yang. “UAV-enabled wireless power transfer with base station charging and UAV power consumption”. In: *IEEE Trans. Veh. Technol.* 69.11 (Nov. 2020), pp. 12883–12896.
- [21] Y. Zeng and R. Zhang. “Energy-efficient UAV communication with trajectory optimization”. In: *IEEE Trans. Wireless Commun.* 16.6 (June 2017), pp. 3747–3760.